

BRENO TOTTI MAIA^{1,2}, CAIO NOGUEIRA ARAUJO DINIZ², GUSTAVO GERMANO PEREIRA², RAISSA SALGADO², ROBERTO PARREIRAS TAVARES²

BOF COLD MODEL - METAL SLAG BATH MASS MOVEMENT DETERMINATION BY SUPERSONIC BLOW FROM MULTI NOZZLES

Abstract

The primary control tool of the BOF process lies on the adjustment of the oxygen blow parameters. The best process conditions involve several variables, like oxygen flow rate, distance bath lance (DBL), number of holes for the oxygen blow, among other factors. Through a visual inspection of the jet penetration and the volume of stagnant zones, the behavior of each configuration tested was analyzed using different sets of nozzles (3 to 6 holes), and with constant distance bath lance (DBL) and flow rate. The analysis of the interaction parameters between the oxygen blow, the molten metal and slag, represented respectively by water and paraffin oil, is the main objective of the present work. It was necessary to develop a new methodology in order to determine the penetration, propose a new formula and adjust the empirical constant, called K factor. The highest penetration were achieved for the nozzles with 3 and 4 holes. The lowest penetration and the highest volume of stagnant zones were represented for the configuration of 6 holes.

Keywords

BOF; Cold Model; Jet Penetration; Stagnant Zones; K Factor

¹ Lumar Metals Ltda. Rod. MG 232, km 09, N° 100, Santana do Paraíso, MG, Brazil, ZIP Code: 35.167-000

² Universidade Federal de Minas Gerais (UFMG), Av. Antônio Carlos, 6627, Belo Horizonte, Minas Gerais, Brazil ZIP Code: 31.270-901

1. Introduction

The steel making process using LD converter (Basic Oxygen Furnace - BOF) represents the most used industrial process for the steel production. Against many challenges, new technologies and industrial techniques have been created in order to make the process more competitive and economically viable. According to Seshadri[1], experimentation methods in the steel making plant represents high costs and may cause problems like breaking of the operational routine, low productivity and dangerous risk to the process. Using physical modelling techniques was possible to recreate converter models in small scale with low costs when compared to industrials experiments. The cold model results are possible to be used in industry when it has similarity between cold model and the prototype and also between the dimensionless numbers, that are important parameters to validate similarity. The fluid dynamics phenomena that happens inside the converter has high complexity, especially due to the interact gas-metal-slag. The Figure 1 shows some phenomena resulting from the interaction.

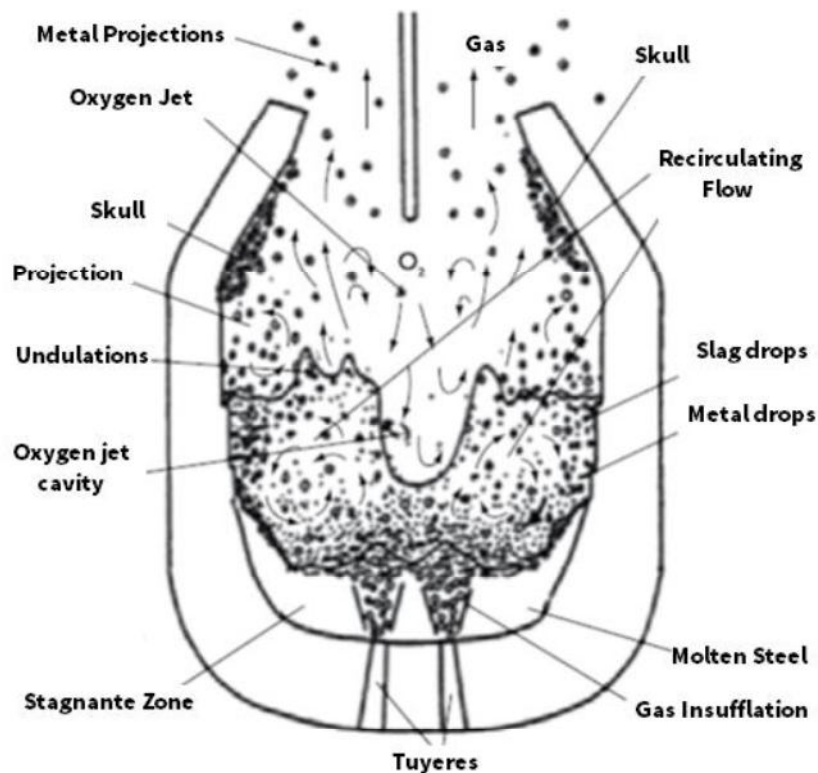


Figure 1: Phenomena resulting from the interaction metal-gas-slag.

About 60% of heat time in the converter is linked to the oxygen blow, which represents an operational key factor in the primary steelmaking. Decreasing blow time results in higher productivity and lower costs. Aiming to decrease the blow time, this study was carried on changing blow nozzles settings in a BOF cold model. The interaction of air jet with the liquid bath (composed of water and paraffin oil, representing steel and slag) was analyzed to get best conditions to the process.

2. Methods and Materials

2.1 Physical modelling

An acrylic model was used to perform the simulations, which simulates a 220 tons converter, localized in the Process Simulation Laboratory - UFMG (LaSiP - Department of Metallurgical Engineering). The dimensions are shown in Figure 2.

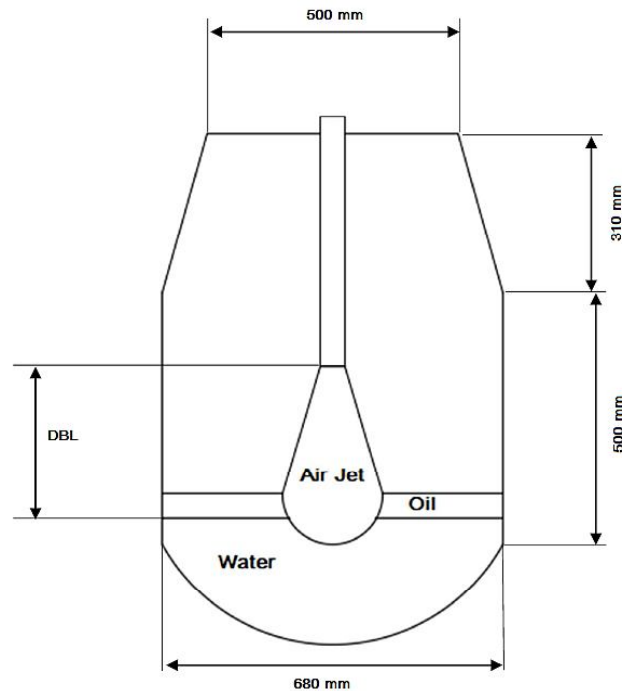


Figure 2: Physical model dimensions of the converter

Before running the test, the vessel has water at the height that represents the level of liquid metal and oil mixed with washing powder until the height that represents the level of slag. At the compressed air system outlet the lance tips were connected. To feed the system with compressed air was used a 22.5kW compressor, capable of providing a maximum pressure of $7.87 \times 10^5 \text{ Pa}$ and a maximum flow of $189 \text{ m}^3/\text{h}$. The bath lance distance and the blow rate were 380 mm and $130 \text{ m}^3/\text{h}$ respectively, for all the simulations, changing just the number of holes, between 3, 4, 5 and 6 holes with angles of 8, 10, 15 and $17,5^\circ$ respectively. The internal geometry of the nozzle is composed by a convergent section and then a short section, where is localized the critical diameter, and at the end a divergent section, as shown in Figure 3.

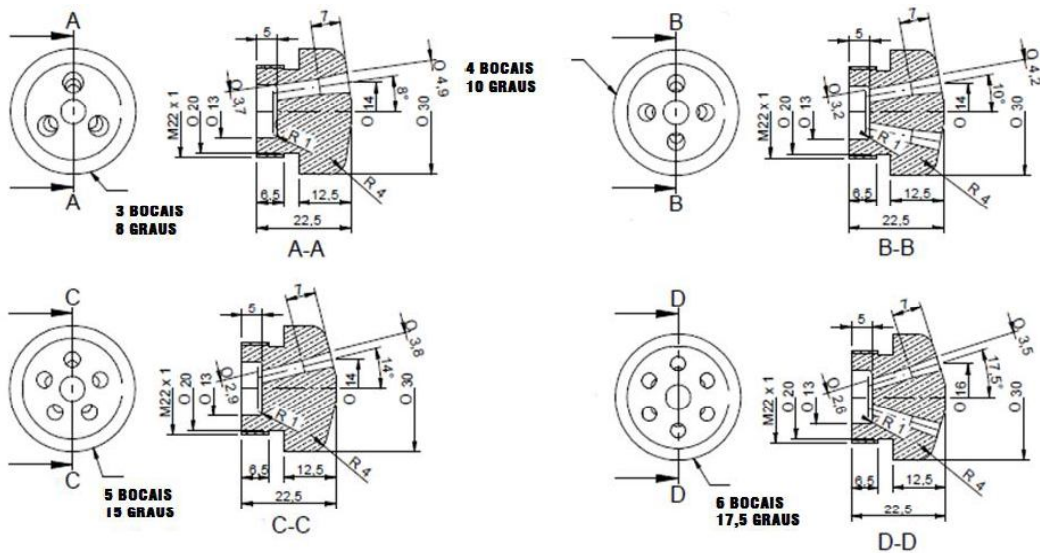


Figure 3: Nozzles internal geometry

Aiming the best conditions to simulate the primary steelmaking, paraffin oil and water were used to represent slag and steel, respectively. Those fluids have been selected because they have physical similarities with steel and slag, thus being able to engender a good dynamic similarity between the experiments and the industrial process [4]. Table 1 shows the comparison between the dimensionless numbers used for dynamic similarity between the cold model and industrial practice.

Table I – Dimensionless Numbers

		Industrial	Model
Fr*	Froude Modified	0,069	0,164
Re*	Reynolds Modified	$6,936 \cdot 10^5$	$1,055 \cdot 10^5$
We*	Weber Modified	$4,771 \cdot 10^3$	$1,370 \cdot 10^3$
Ma	Mach Number	2,07	1,79

2.2 Methods

To perform the experiments, the physical model is filled with water to a distance of 250mm from the bottom, and then the air jet is released to adjust the flow to $130 \text{ m}^3 / \text{h}$. With the flow rate set by the first air outlet valve, closes the second valve. From the moment that the bath is stable, add a layer of 30mm paraffin oil, which quickly separates from water, yielding a clear distinction between phases, as shown in Figure 4.



Figure 4: Separation between the phase's water and oil, a) original; b) contrasted

150g of Brillhante[®] washing powder is added to the bath, which is responsible for generating an emulsion during the blowing, aiming to reproduce the typical emulsion that happens during decarburization in the BOF converter. Two cameras were positioned to record the bath behavior in contact with air jet. Two reflectors were placed on the back of the model, thus generating better contrast for recording.

2.3 Measure of jet penetrations and mixed volume

In order to edit the videos, was used the Movie Studio Platinum software, which enabled the recording of images. From the moment that starts the blowing, the images were captured at each 5 seconds, making possible to get all the data of penetration and mixed volume. Using the recorded images, was created a contrast through GIMP[®] software, enabling an accurate result of measured values. In order to measure the penetration of air jet in the bath and the displaced volume the ImageJ[®] software was used. The figure 5 shows the method to measure the penetration in the recorded images.

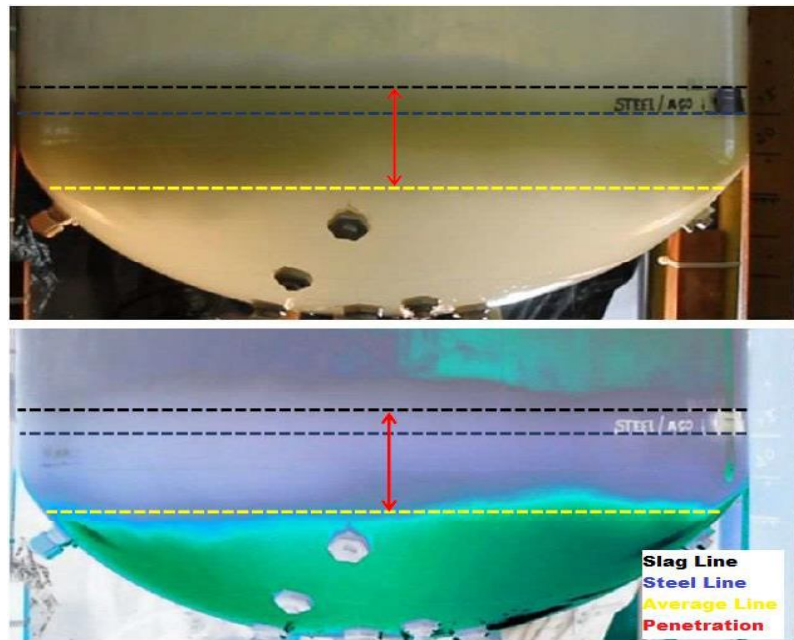


Figure 5: Definitions of the Slag Line, Steel Line, Average Line and Penetration for: a) original image; b) contrasted image

Figure 5 shows the pre-established concepts for measuring penetration: the slag line, steel line, average line and penetration. The slag and steel lines represent the levels of paraffin oil (slag) and water (steel) respectively. The middle line represents the average end point of the jet penetration. The acquisition of penetration data were obtained with a gap of 5 seconds for each value. For the same time gap, data were collected in order to analyze the percentage of stagnant bath and thereby calculate the mixed volume, as shown in Figure 6.

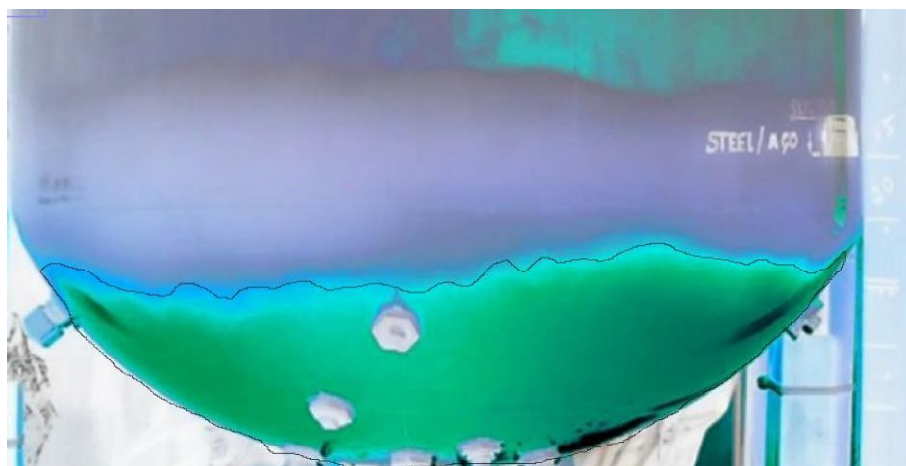


Figura 6: Stagnant volume delimited using the software ImageJ®

2.4 Factor K

According to Maia [3], is possible to relate the number of oxygen outlet holes with the jet penetration value in the bath, through a specific equation for the liquid biphasic system. In this equations, an evolution of other studies [5- 10] considers the surface tension of slag and steel layers, considering the direct effect of those parameters in the jet penetration, as shown in equation 1.

$$\frac{1}{K^2} \times \left(\frac{\pi}{2} \times \frac{P}{(DBL + P)} \right) \times \left(1 + \frac{1}{P^2} \times \frac{\cos \theta \times (\sigma_{STEEL} + \sigma_{SLAG})}{(\rho_{STEEL} + \rho_{SLAG}) \times g} \right) = \left(\frac{\pi}{4} \times \frac{(\rho_{GAS} \times V_{EXIT}^2 \times D_{EXIT}^2 \times \cos \theta^2 \times n)}{(\rho_{STEEL} + \rho_{SLAG}) \times g \times (DBL + P)^3} \right)$$

Equation 1

Where “K” is an empirical constant, “DBL” – bath lance distance (m), “P” – cavity penetration inside de bath (m), “ ρ_{steel} ” – bath density (kg.m^{-3}), “ ρ_{slag} ” – slag density (kg.m^{-3}), “ ρ_{gas} ” – gas density (kg.m^{-3}), “ σ ” – surface tension (N.m^{-1}), “ V_{exit} ” – exit velocity (m/s), “ D_{exit} ” – exit diameter, “g” – gravity acceleration (m.s^{-2}), “ θ ” – inclination angle and “n” number of holes in the nozzle .

The penetration data were analyzed for 04 viewers in different ways and thus obtaining mean values and standard deviation of the data. From the penetration values obtained, was possible to get the value of K for each test setup.

3. Results and Discussions

3.1 Jet Penetration

The analysis the images, made it possible to estimate the values of penetration during the air blow. It was noticed that this value is not constant throughout blowing time, so the air jet gradually displaces down a greater volume of the water, oil and soap.

Figures 7, 8, 9 e 10 illustrate, in a comparative way, the bath behaviour for the first 20 seconds of blowing, for each test configuration. The blue/green contrast volume represents the bath stagnant zones.

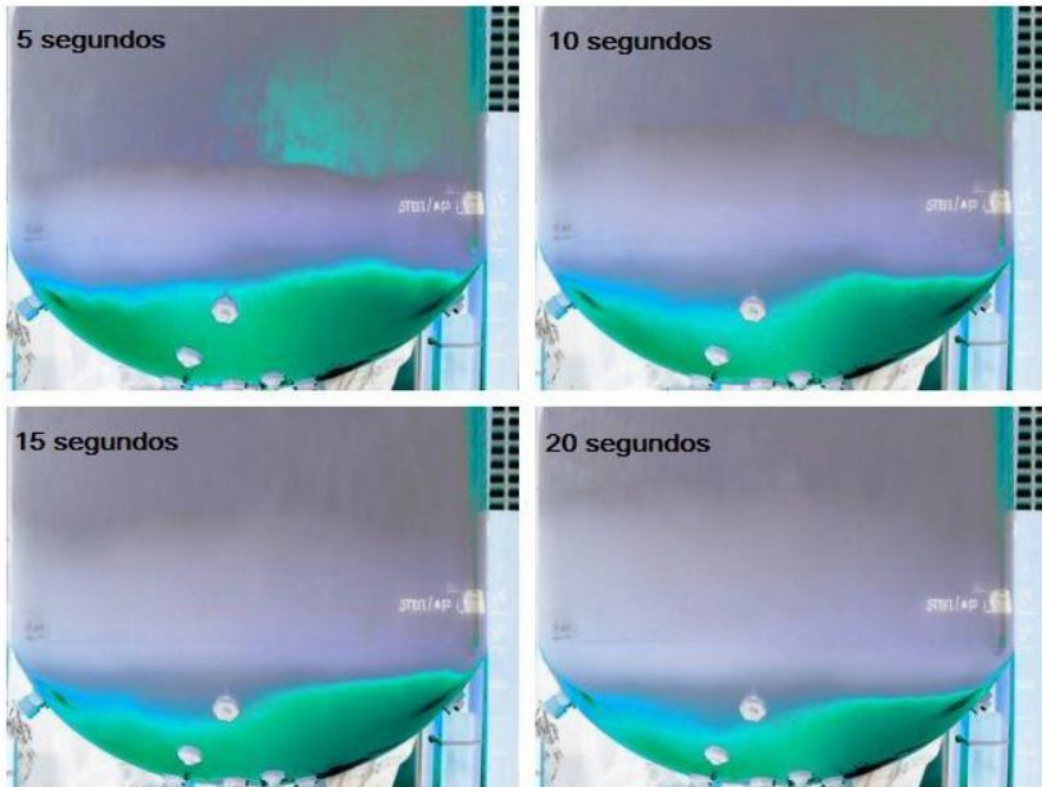


Figure 7: First 20 seconds of blow, configuration of 3 holes nozzle.

For the test configuration illustrate on Figure 7, as the jet penetrates the mixture, the generated emulsion increases uniformly, stabilizing along with the penetration.

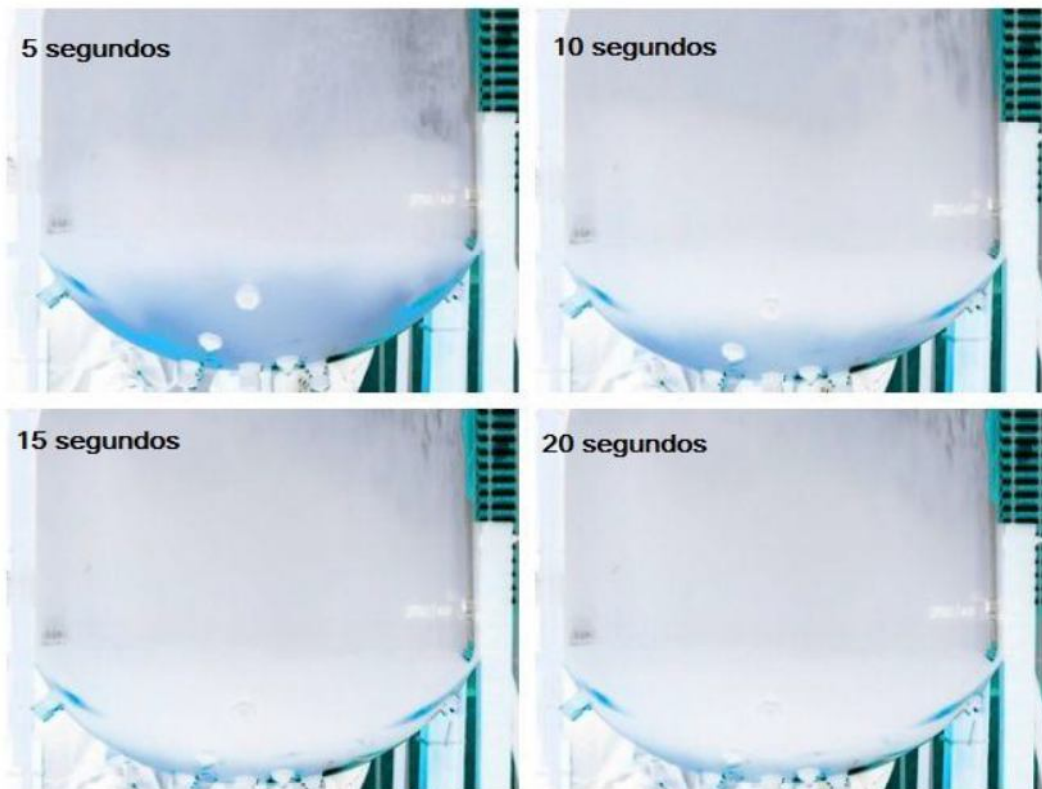


Figure 8: First 20 seconds of blow, configuration of 4 holes nozzle.

Figure 8 illustrates the 4 holes nozzle test, in which the highest penetration values were registered. The concentrated jet quickly touches the bottom of the cold model, making the green/blue areas, which represents the stagnant zones, disappear and the whole bath was taken by the mixture.

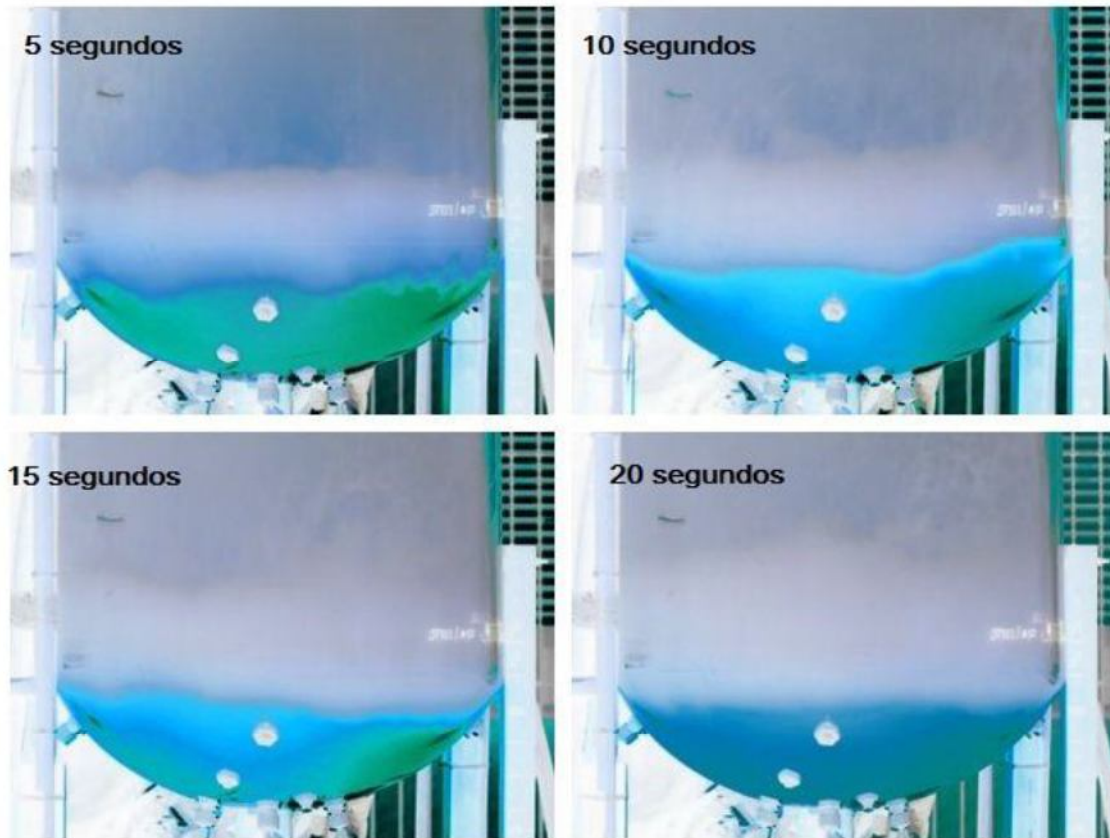


Figure 9: First 20 seconds of blow, configuration of 5 holes nozzle.

For the 5 holes nozzle test, it is possible to notice that the air jet penetrates the bath more slowly when compared with the tests of Figures 7 and 8, generating, in a uniform mode, an emulsion that grows as the air jet penetrates increasingly the bath, until the moment that both the jet and the emulsion stabilize.

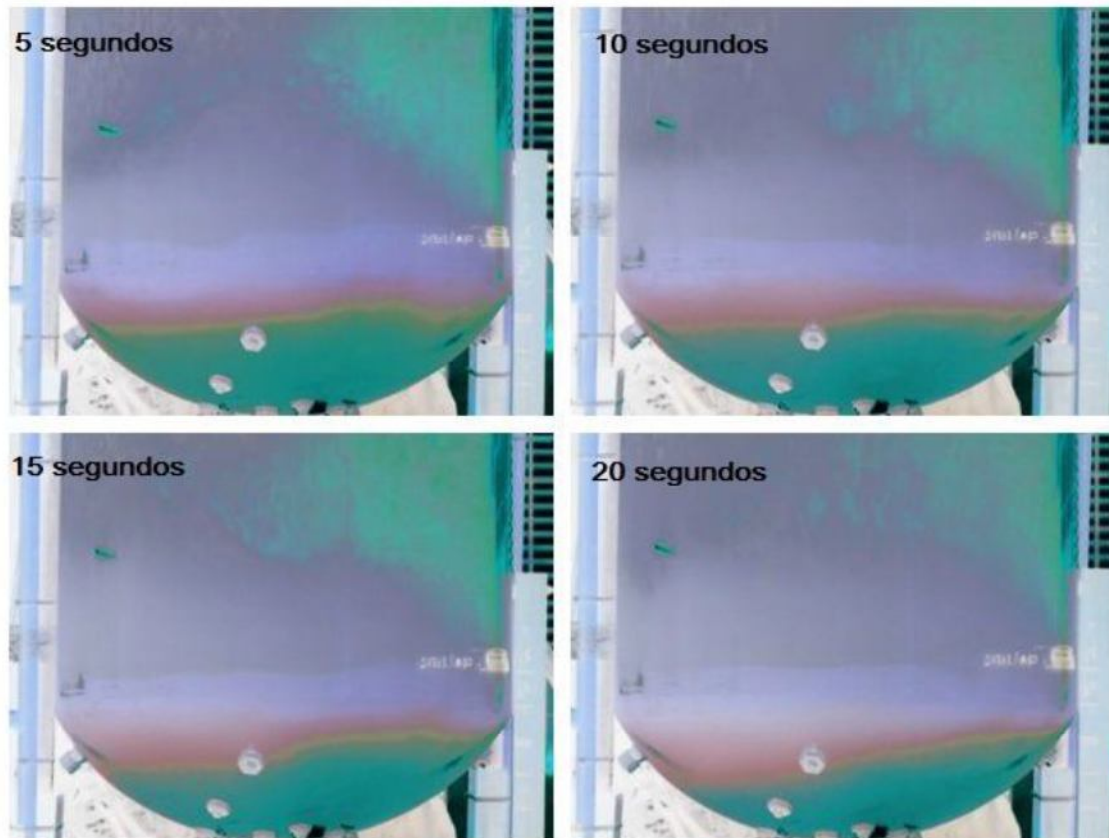


Figure 10: First 20 seconds of blow, configuration of 6 holes nozzle.

Figure 10 illustrates the 6 holes nozzle test, which registered the the lower value of penetration. The jet achieve a small penetration value, stabilizes quickly and generate a little quantity of emulsion, when compared with the other tests. The direction of bath rotation is counter clockwise.

After the analysis of the realized tests, it was possible to notice that higher penetration values lead to a reduction in the impact area between jet and bath, dimple, which characterizes a hard blow, that is used for decarburization. The 3 and 4 holes tests presented a bigger splash when compared to the 5 and 6 holes tests. The configuration of the 6 holes nozzle registered the smaller splash, characterizing a jet with a bigger dimple and less projections.

Figure 11 illustrates the jet being despatched over the bath, for the 3 holes nozzle configuration, in which the air jet firstly encounters the oil layer, which provides resistance to jet penetration when compared with water.

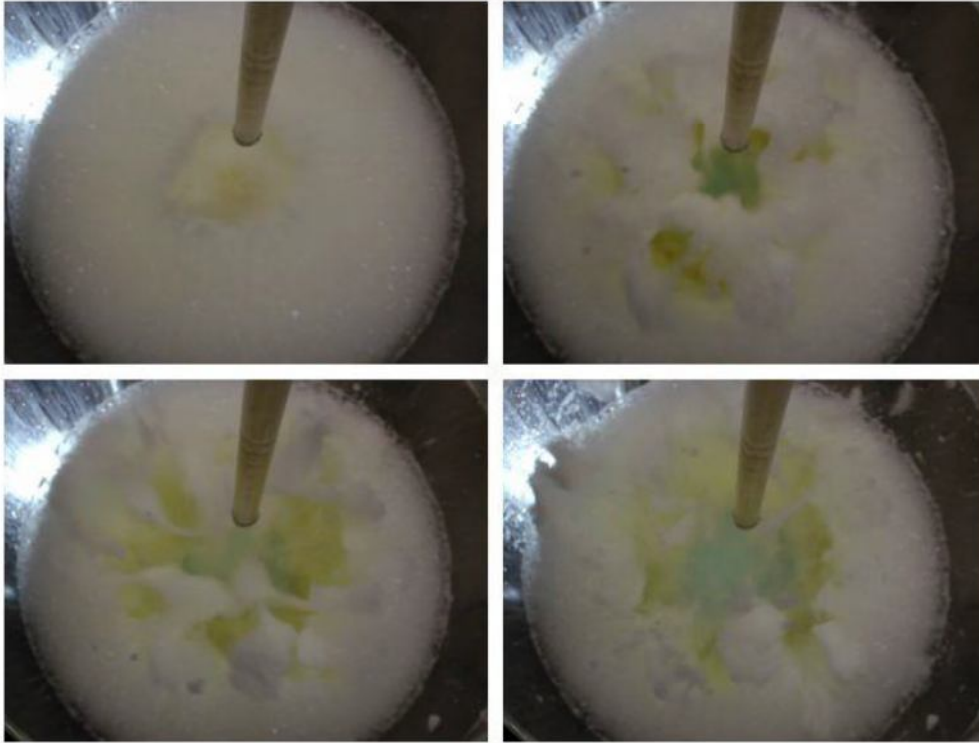


Figure 11: Initial air jet impact in the bath.

In figure 11, the jet interacts with the oil layer and a small fraction of water, enough to generate emulsion caused by the powder soap. Then, gradually the paraffin oil layer is displaced in the radial direction, exposing the bath. Therefore, finally the jet penetrates the water layer forming a dimple not noticed in a side view. The emulsion is directed onto the walls of the model. With the paraffin oil layer is possible to notice a considerable reduction of splashing water, symbolizing the metal projections. This result is similar to that presented by Li et al^[11]. For the configurations that presented lower penetration values, it was noticed a dimple expansion, characterizing a soft blow, which is used for dephosphoration in the primary refine and may potentially represent an attack to the trunnion lines. This behaviour was observed for all the configurations, but the intensity of the phenomena was different.

Different penetration values were found for the four different test configurations (nozzles with 3, 4, 5 e 6 holes), as represented by Figure 12.

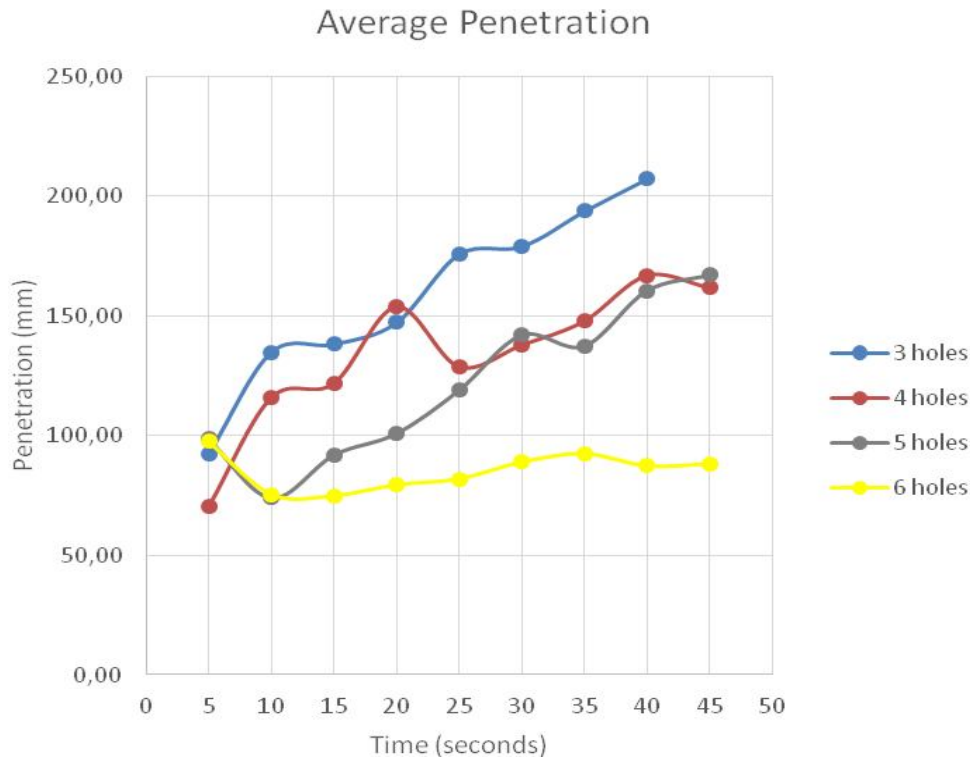


Figure 12: Average Penetration x Time, for the nozzle configurations with 3, 4, 5 e 6 holes.

The analysis of the above plot allows the verification of distinct behaviours for the different nozzle configurations, so that for the nozzles with 3 and 4 holes the penetration is bigger when compared with nozzles with 5 and 6 holes. The following analysis was carried out for each configuration, based on the filming carried out and on the graph presented on Figure 12. The goal was to describe the behaviour of the air jet penetration in the bath for the nozzle configurations used in the tests.

i. 3 holes

The value of jet penetration clearly increases with time. This behaviour can be explained by the bigger dynamic viscosity presented by the paraffin oil (0,055Pa.s) when compared with water (0,001 Pa.s). After breaking the barrier created by the oil and emulsion layer, the jet can penetrate the water more easily, generating higher penetration values.

ii. 4 holes

High penetration values were observed for a 4 holes configuration but, for the most part, smaller than the 3 hole configuration. With the time analyzer, the penetration values tend to be maxima controlled by the 3hole test, but taking a longer time interval.

iii. 5 holes

There is a progressive behaviour of penetration similar to the 3 holes configuration, but with smaller values. The air jet firstly overcome the oil and emulsion barrier, penetrating the water and stabilizing.

iv. 6 holes

In this configuration it is noticed a regular behaviour, in which there is no big value of penetration in the bath when compared with other configurations. The air blow shown for the 6 holes nozzle presents a bigger impact area over the bath, dimple and, thereafter, a lower energy for the penetration, so that the bath stabilizes quickly, without big variations.

3.2 Displaced Volume

There is a volume in the bath that stays stagnant, without get mixed up with the emulsion generated by water oil and powder soap, as shown in Figures 7, 8, 9 and 10. This volume decreases progressively as the jet penetrates the bath, until the moment that the jet becomes stable.

Figure 13 presents a graph with the behaviour of the mixed volume (total volume – stagnant zones volume) versus time, for each nozzle configuration.

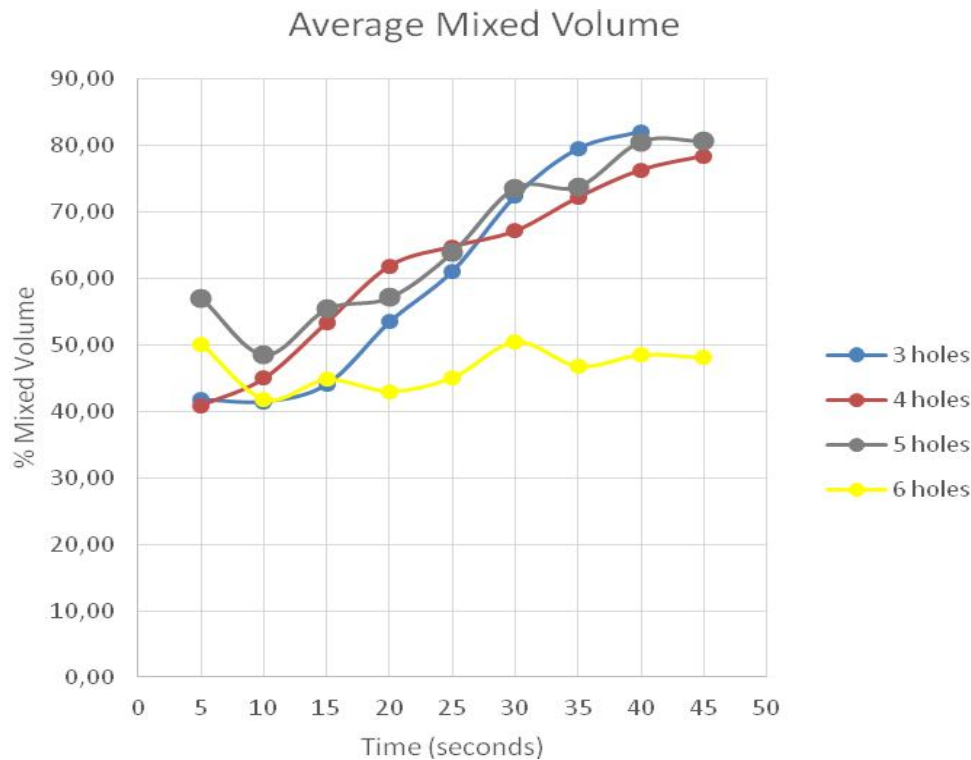


Figure 13: % Mixed x Time for the nozzles with 3, 4, 5 and 6 holes

From the observation of the Figure 13, it is possible to notice a progressive increase of the mixture volume with time, similar to what happens with the air jet penetration in the bath. The graph shows a similar initial behaviour for the nozzles with 3, 5 and 6 holes. The 4 holes configuration has a different behaviour. For this configuration, the jet quickly touches the bottom of the model, as previously mentioned, which leads to a high velocity of bath mixture, eliminating promptly the stagnant zones. The stable behaviour of the nozzle with 6 holes can be explained by the small penetration value, which generates less bath agitation when compared to the other configurations and consequently a high volume of stagnant zones. The configurations of 3 and 5 holes presents a progression of mixture volume, so that the stagnant zones decreases with time until a value that they become constant.

3.3 K factor

A constant K was calculated for each value obtained by equation 1. Based on penetration results the K value varied according to the time for the most configurations. Figure 14 shows the average K for holes with 3, 4, 5 and 6.

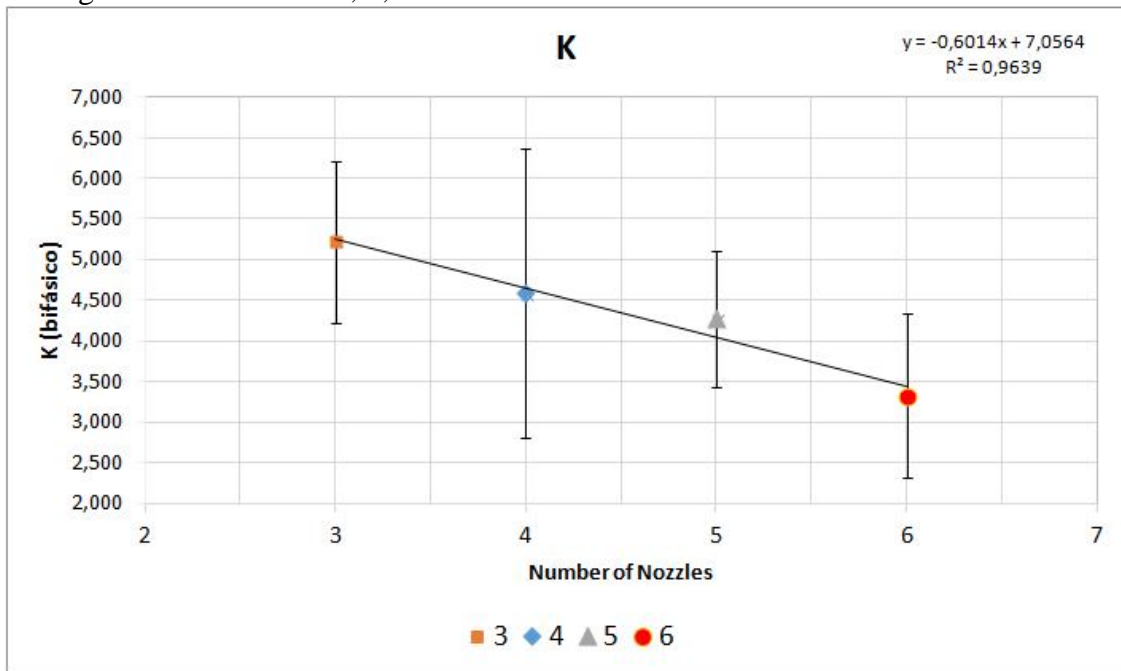


Figure 14: Average K x Number of holes

The data of all time gaps were considered for k factor calculations. The stability definition was not clear for viewers, even getting as answer the increase of standard deviation. Results of graphic 14 provided the K value tends to decrease with increasing nozzles number. Only the configuration of 4 holes presented high K value, but it was not the expected behavior. This value can be explained due to high jet penetration that happens in a concentrated mode and with small dimple, tapping the bottom of the cold model.

Calculated values are considerably lower than results obtained by Breno et al^[10], which only used water in the experiments, not considering the slag effect and emulsion produced in process. The table II shows “K” values for tests with paraffin oil, water and washing powder in comparison to that realized only using water (K’).

Table 2 – Comparison between tests with and without oil.

Number of holes	K (oil + water)	K' (water)
3	5,225	5,769
4	4,583	5,042
5	4,267	4,663
6	3,325	4,418

The addition of an oil layer on bath explains the difference between values of K and K’, being K the new value of empirical constant for test with paraffin oil and water and K’ for tests

conducted only using water. When the air jet reaches the oil layer, it is deadened, loses energy and reduces penetration. The new results are more representative than the experiments using just the water phase.

4. Conclusions

The main conclusions of the study are:

1. The oil layer added to bath, that simulates the slag, produces decrease of penetration value in comparison to tests carried out only with water;
2. For nozzles with lower holes number, there is a higher jet penetration value on bath;
3. Jets with lower penetration value produce less agitation on bath, creating a high volume of stagnant zones;
4. Values of K tend to be lower for nozzles with more numbers of holes;
5. Values of K significantly decrease for tests using oil as the slag layer.

Acknowledgments

The authors thank the Universidade Federal de Minas Gerais for providing the dependencies of Process Simulation Laboratory - UFMG (Lasip) and inputs for the tests and the Lumar Metals by encouraging continued research and support.

References

- 1 SESHADRI, V., TAVARES, R. P., SILVA, C. A., SILVA, I. A., Fenômenos de transporte: Fundamentos e aplicações nas Engenharias Metalúrgica e de Materiais; São Paulo; Associação Brasileira de Metalurgia, Materiais e Mineração, 2010; 812 p.
- 2 ALMEIDA, L. P. *et al.* Effects of some operational parameters upon degaseification rate, mixing time, splashing and skull development in a combined-blow converter during steelmaking refining: a physical model approach. In: AISTech 2010 –THE IRON & STEEL TECHNOLOGY CONFERENCE AND EXPOSITION, 2010, Pittsburgh. *Proceedings...* Warrendale, PA: AIST, 2010. p. 274-85.
- 3 MAIA, B. T., *Modelamento Físico e Matemático do Escoamento de Fluidos nos Processos BOF e EOF*: Escola de Engenharia da UFMG, 2013. (Dissertação, Doutorado em Engenharia Metalúrgica e de Minas).
- 4 BARBOSA, F. A., *Modelamento Matemático e Físico do Escoamento do Aço Líquido em Diferentes Projetos de Distribuidor do Lingotamento Contínuo da USIMINAS*. Belo Horizonte: Escola de Engenharia da UFMG, 2002. 188p. (Dissertação, Mestrado em Engenharia Metalúrgica e de Minas).
- 5 SZEKELY, J. THEMELIS, N. J., *Rate Phenomena in Process Metallurgy*. 1 ed. Montreal: John Wiley & Sons, 1971. 784p.
- 6 MEIDANI, A. R. N., ISAC, M., RICHARDSON, A., CAMERON, A., GUTHRIE, R. I. L. Modeling Shrouded Supersonic Jets in Metallurgical Reactor Vessels. *ISIJ International*, 2004, v.44, n.10, p. 1639-1645.
- 7 ALAM, M., IRONS, G., BROOKS, G., FONTANA, A., NASER, J., Inclined Jetting and Splashing in Electric Arc Furnace Steelmaking. *ISIJ International*, 2011, v.51, n.9, p. 1439-1447.

- 8 MAIA, B. T., IMAGAWA, R. K., BATISTA, C. J., PETRUCELLI, A. C., TAVARES, R. P. Effects of Blow Parameters in the Jet Penetration by Physical Model of BOF Converter. AISTech 2013 Proceedings. Stoughton, 2013. p.2059-2073.
- 9 MAIA, B. T. FAUSTINO, R. A., ABREU, G., COSTA, B., TAVARES, R. P., Efeitos dos Parâmetros de Sopros no Tempo de Mistura Utilizando Modelo Físico de Convertedor. Anais do 44º Seminário de Aciaria Internacional, Araxá, Minas Gerais, Maio, 2013.
- 10 MAIA, B. T., PETRUCELLI, A. C., DINIZ, C. N. A., SILVEIRA, D., ANDRADE, P. H. M. S., IMAGAWA, R. K., TAVARES, R. P., Comparação da Penetração do sopro de Oxigênio em Convertedores BOF com Bicos Multifuros utilizando Modelagem Física. Seminário de Aciaria Internacional. Porto Alegre, Maio 2014.